Recent Results in Exotic and Electroweak Physics from the Tevatron

Dave Toback

University of Maryland
for the CDF and DØ Collaborations

Abstract

As the Fermilab Tevatron and CDF and DØ detectors prepare for Run II, a large number of new results using Run I data continue to come out which search for hints of physics beyond the Standard Model. Many of these results place direct restrictions on the production of new particles while other are precision measurements of many of the SM parameters. This talk describes a two such sets of new results; one set directly search for second generation leptoquarks and a second set which make precision Electroweak measurements of the masses, widths and cross sections of the massive vector bosons.

1 Introduction

As the Fermilab Tevatron and CDF and DØ detectors prepare for Run II, a large number of new results using Run I data continue to come out which search for hints of physics beyond the Standard Model. Many of these results place direct restrictions on the production of new particles while other are precision measurements of many of the SM parameters. This talk describes a two such sets of new results; one set directly search for second generation leptoquarks and a second set which make precision Electroweak measurements of the masses, widths and cross sections of the massive vector bosons.

The apparent symmetry between leptons and quarks has suggested the existence of leptoquarks (LQ) in many extensions of the Standard Model [1]. These hypothetical particles carry QCD color, fractional electric charge and both lepton and baryon number. Since there are stringent limits on flavor changing neutral currents, LQ are expected to only couple within a single generation [2]. We report on a set of direct searches for second generation leptoquarks in various decay channels. Improvements in searching methods have greatly extend the current sensitivity. In addition many results are combined to further extend the sensitivity. These results also place severe restrictions on the production of vector leptoquarks.

The Tevatron experiments continue to make precision measurements of QCD and Electroweak parameters. Current measurements are sensitive to large deviations from SM expectations which might be indicative of physics beyond the SM. Increased sensitivity will eventually tightly constrain the Higgs and SUSY sectors or eliminate them as possible descriptions of the world. In addition, a full understanding of the electroweak sector allows for more effective searches. We report on a set of new measurements of the W width, the W and Z cross sections, and new precision measurements of the W mass. All are comparable to or are the most precise in the world.

2 Second Generation Leptoquarks at the Tevatron

At the Tevatron, leptoquark production is assumed [3] to be dominated by $p\bar{p} \to g + X \to LQ\overline{LQ} + X$. Since there are already severe limits on the production and decay of first generation LQ we have searched for LQ which couple to the second generation. The decay of a second generation LQ is either through $LQ \to \mu q$ (branching ratio β) or $LQ \to \nu q$ (branching ratio 1-β). Thus, there are three final state signatures: $LQ\overline{LQ} \to \mu\mu qq \to \mu\mu jj$ (Br $= \beta^2$), $LQ\overline{LQ} \to \mu\nu qq \to \mu \not{E}_{\mathrm{T}} jj$ (Br $= 2\beta(1-\beta)$), and $LQ\overline{LQ} \to \nu\nu qq \to jj \not{E}_{\mathrm{T}}$

(Br = $(1-\beta)^2$).

2.1 CDF Results in the 2 Muons and 2 Jets Channel

The CDF detector (described in [4]) has published a search [5] for second generation LQ in the $\mu\mu jj$ channel using 110 pb^{-1} of data. Candidate events are required to have two isolated muon candidates, one with P_T>30 GeV, and a second with P_T> 20 GeV and $|\eta| < 1.0$. Events with $\mu\mu$ masses consistent with Z^0, J/ψ and υ production are removed. In addition each candidate events is required to have two jets, one with P_T>30 GeV, and a second with P_T> 15 GeV, both with $|\eta| < 2.4$. Next the jets and muons in each event are paired such that their invariant masses are most similar (see Figure 1). To set limits for a given LQ mass events are selected in a 3σ region around the hypothetical LQ mass and compared to background predictions (dominated by Drell-Yan, WW and $Z \rightarrow \tau\tau$ production). There is no evidence for an excess and 95% C.L. cross section limits are shown in Figure 2. Mass limits require M_{LQ} >202 and 160 GeV for $\beta = 1.0$ and 0.5 respectively.

2.2 New DØ Results

The DØ detector (described in [6]) has also searched for second generation LQ in 94 pb^{-1} of data. This search extends the previous measurements by looking in both the $\mu\mu jj$ and $\mu\nu jj$ channels. In addition new optimization techniques using Neural Nets are employed. Also, cross section limits are interpreted as mass limits on both scalar and vector leptoquarks. Finally, the various DØ results, including those from the $\nu\nu$ channel, are combined to set limits on the mass of the LQ as a function of β.

2.2.1 $\mu\nu$ + Jets

The DØ $\mu\nu jj$ search, described in Ref [7] accepts candidates with one isolated Muon with $P_T > 25$ GeV, $|\eta| < 0.95$, a neutrino (identified using $\not\!\!E_T$in the calorimeter) > 30 GeV and 2 or more jets with E_T> 15 GeV,$|\eta_1| < 1.5$ and $|\eta_2| < 2.0$. In addition, there are two topology cuts: $\Delta\phi_{\mu\nu} > 0.3$ $\Delta R_{jj} > 1.4$.

A total of 107 events pass the requirements. The dominant backgrounds are $W + 2$ Jets (106 ± 30 events), $Z + 2$ Jets(2.7 ± 0.7 events), $t\bar{t}$(2.4 ± 0.8 events) and WW(1.5 ± 0.6 events) and predict a total of 108± 30 total events in the data. The data are

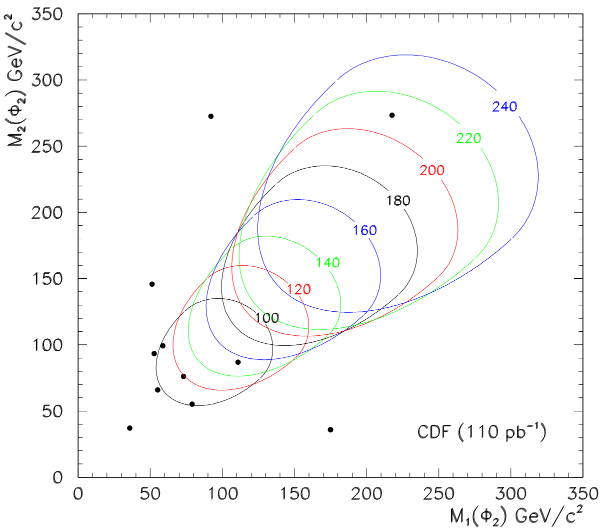

Figure 1: The invariant mass of μj combinations in the CDF second generation leptoquark search. A total of 11 events candidates are displayed. The ovals are acceptance region for various LQ masses.

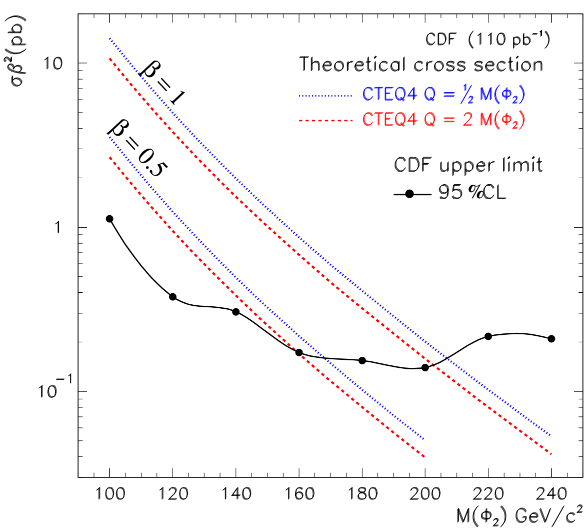

Figure 2: The 95% C.L. cross section upper limits on second generation leptoquark from the CDF detector. The superimposed lines are the theoretical predictions for scalar LQ. From the intersection of the lines, mass limits require M_{LQ} >202 and 160 GeV for $\beta = 1.0$ and 0.5 respectively.

shown in Figure 3 along with the background expectation and the expectations from a scalar leptoquark with $M_{LQ} = 160$ GeV. No evidence of a signal is seen. To set limits, an optimization technique is employed using neutral networks (NN) [8]. The network is trained, using Monte Carlo events, to separate signal and background on an event by event basis. It returning a single value (D_{NN}) near 0 if the event is background like, and a number near 1.0 if it is signal like. The results for the $\mu\nu jj$ data set are shown in Figure 4. A optimization technique which, on average, gives the best limit is used to determine the final cut on the NN output. This cut is set at $D_{NN} > 0.9$.

2.2.2 $\mu\mu$ + Jets

The DØ $\mu\mu jj$ search, described in Ref. [9] is similar to the $\mu\nu jj$ search except that it requires two muons and no missing transverse energy. Specifically, it accepts candidates if they contain 2 isolated muons with $P_T > 20$ GeV, $|\eta| < 1.7$ and 2 or more jets with

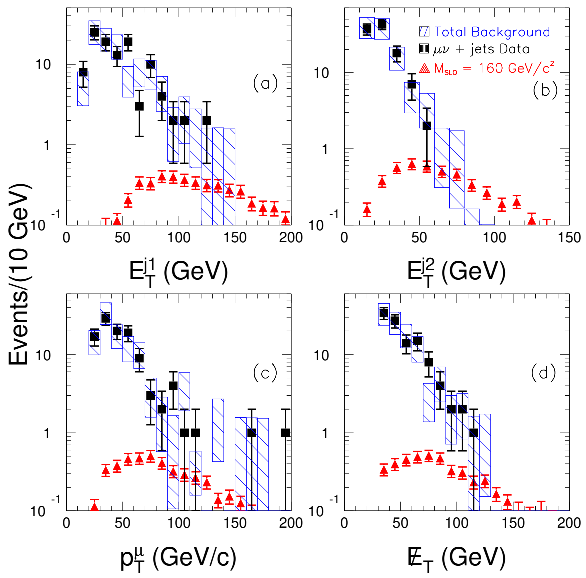

Figure 3: Kinematic distributions for the $\mu\nu + jets$ events in the DØ second generation LQ search. The quantities in (a)-(d) are used as inputs into the neural network. The shaded regions give the background expectations. The points are the data and the triangles are the prediction for a 160 GeV scalar LQ.

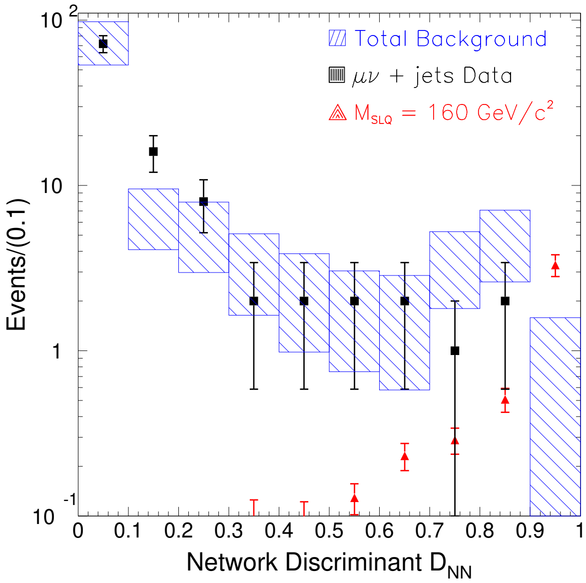

Figure 4: Output of the neural network for the data, backgrounds and signal predictions in the DØ second generation LQ analysis in the $\mu\nu jj$ channel. The network calculates a value for each event based on the inputs (shown in Figure 3).

$\mathrm{E_T} > 20$ GeV, $|\eta| < 3.0$. In addition there is sphericity > 0.05 requirement.

A total of 53 events passing the above requirements are observed in the data. The dominant backgrounds are W + Jets (43 ± 13 events), Z + Jets (5.6 ± 0.9 events), WW (2.3 ± 0.9 events), and $t\bar{t}$ (2.1 ± 0.6 events) for a total of 53 ± 13 events. These events are shown in Figures 5 and 6 along with the background expectation and the expectations from a scalar leptoquark with $\mathrm{M_{LQ}} = 200$ GeV. Since no excess is seen, again a neutral network (see Figure 6)is used.

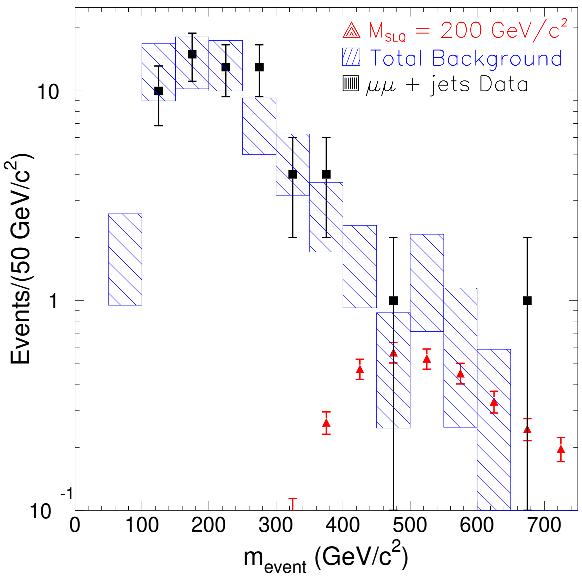

Figure 5: Invariant mass of all muons and jets in the DØ second generation leptoquark $\mu\mu + Jets$ analysis. The shaded regions give the background expectations. The points are the data and the triangles are the prediction for a 200 GeV scalar LQ.

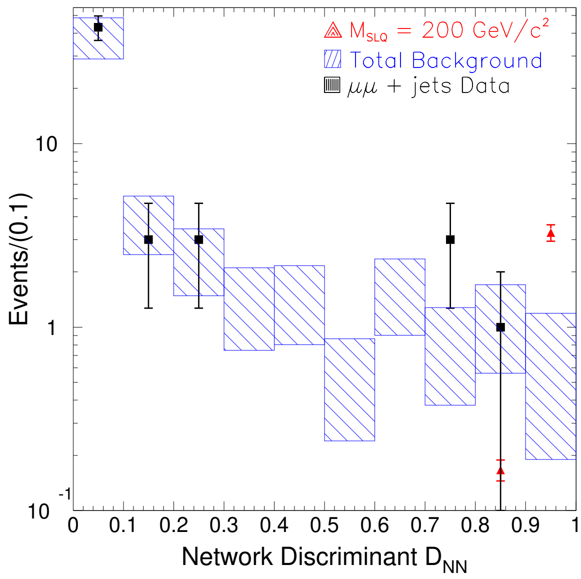

Figure 6: Output of the neural network for the data, backgrounds and signal predictions in the DØ second generation LQ analysis in the $\mu\mu jj$ channel. The network calculates a value for each event based on a number of inputs (one of which shown in Figure 5).

2.2.3 Combined second Generation Leptoquark DØ Results

Since there is no evidence for an excess in either the $\mu\nu jj$ and $\mu\mu jj$ channel limits are set on LQ in both channels. In addition, the results are combined, along with the $\nu\nu jj$ search [10], to produce 95% C.L. cross section limits as a function of β. The results are shown in Figure 7 for $\beta = 1$ and $\beta = 1/2$. In addition to scalar LQ, limits are also set on Vector LQ with Minimal Vector and Yang-Mills couplings [11]. Mass limits for the three models for $\beta = 1.0$, 0.5 and 0.0 are given in Table 1. Mass limits as a function of β are given in Figure 8.

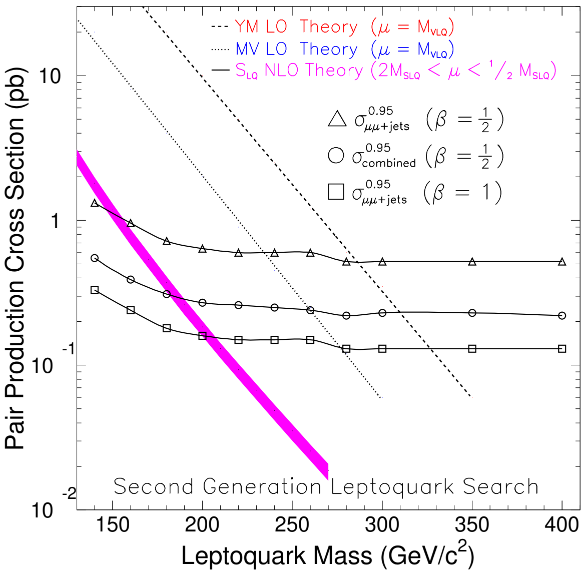

Figure 7: Combined 95% C.L. cross section limits for the DØ second generation leptoquark analyses. Results are shown for the $\mu\mu$ + jets channel for $\beta = 1$, $1/2$, and for the combination of channels at $\beta = 1/2$.

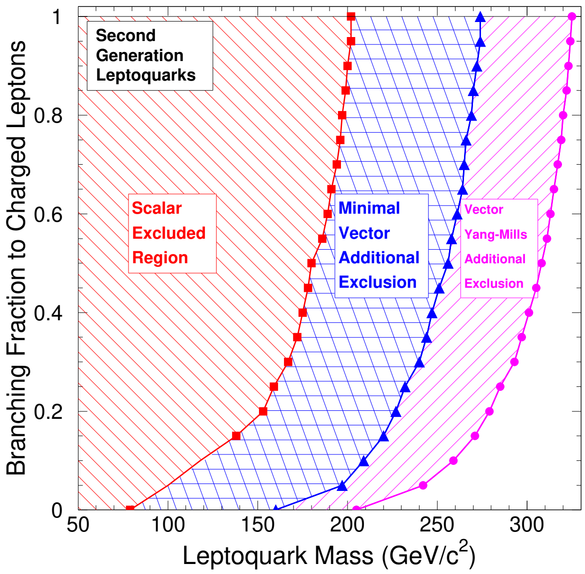

Figure 8: The combined DØ second generation leptoquark mass limits. The region to the left of each curve represents the excluded region in the β - M_{LQ} plane from combining the $\mu\mu jj$, $\mu\nu\, jj$ and $\nu\nu jj$ channels.

Branching Fraction (β)	Scalar Couplings (GeV/c^2)	Mimimal Vector (GeV/c^2)	Yang-Mills Vector (GeV/c^2)
1	200	275	325
1/2	180	260	310
0	79	160	205

Table 1: Table of the combined 95% C.L. mass results for a few points in parameter space for second generation scalar, and vector leptoquarks. The two different types of leptoquarks are Minimal vector and Yang-Mills [11].

3 W and Z Physics at the Tevatron

At the Tevatron, W and Z candidates are typically identified through the selection of events which have decayed into the leptonic final state. For example, large samples of W's and Z's are selected via $W \to e\nu$ and $Z^0 \to e^+e^-$. More specifically, W's are selected by the presence of a 1 single isolated electron, $E_T > 25$ GeV, and $\not{E}_T > 25$ GeV. Z^0 candidates are selected by the presence of 2 isolated electrons with $E_T > 25$ GeV and typically require 75 GeV $< M_{e^+e^-} <$ 105 GeV. It is with these samples that a series of precision electroweak measurements have been made. We begin with two measurements of the W width. We then continue with new measurements of the W and Z cross sections. We conclude with a quick summary of the precision measurements of the W mass.

3.1 Direct W Width Measurement

The width of the W can be directly measured from the lineshape of the W transverse mass spectrum. This measurement is most sensitive to the tail of the Transverse mass distribution as shown in Figure 9. This has recently been measured by the CDF collaboration. The results are shown in Figure 10. The width, with uncertainty dominated by the statistics in the sample above 100 GeV, is measured to be $\Gamma(W) = 2.19 \pm 0.170(stat) \pm 0.090$ (sys) GeV.

3.2 Indirect W Width & Br$(W \to e\nu)$

In Run II the most precise measurement of the W width will come from a direct measurement. However, with limited statistics a more precise measurement of the W width comes from an indirect method. By taking the ratio of the W and Z electronic cross sections one can get much higher statistics and determine the branching ratio of $W \to e\nu$ in the process. In this measurement, the ratio known as R, gives:

$$R \equiv \frac{\sigma(p\bar{p} \to W + X) \cdot Br(W \to e\nu)}{\sigma(p\bar{p} \to Z^0 + X) \cdot Br(Z^0 \to e^+e^-)}$$

$$= \frac{\sigma(W)}{\sigma(Z)} \cdot \frac{\Gamma(Z)}{\Gamma \to (Z \to e^+e^-)} \cdot \frac{\Gamma(W \to e\nu)}{\Gamma(W)}$$

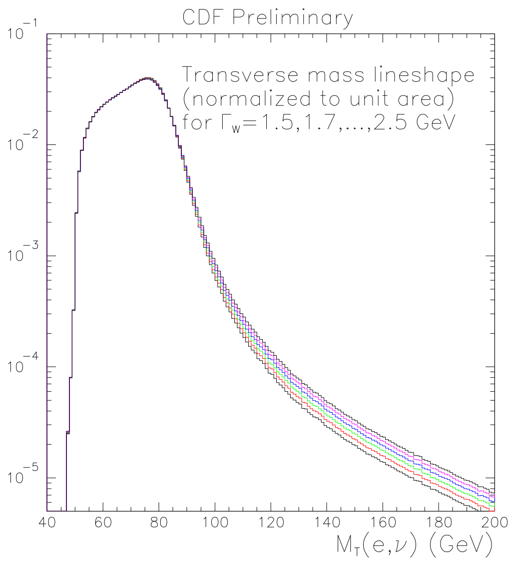

Figure 9: Simulated $\mathrm{M_T}(\mathrm{e},\nu)$ lineshapes, normazized to unit area for $\Gamma(W) = 1.5, 1.7, ...2.5$ GeV. Detector response, kinematic cuts, and fiducial cuts for the CDF detector have been included.

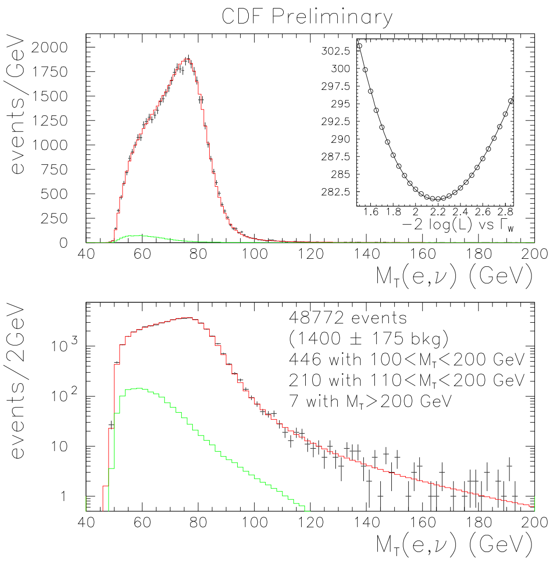

Figure 10: The CDF $W \to e\nu$ data with the best fit of the lineshape overlayed.

$$= \overbrace{(3.29 \pm 0.03)}^{Theory} \cdot \overbrace{(0.03367 \pm 0.00006)^{-1}}^{LEP} \cdot \overbrace{Br(W \to e\nu)}^{Extract}$$

This was measured in Run Ia by CDF [12] with the results $\Gamma(W) = 2.064 \pm 0.084$ GeV and $\mathrm{Br}(W \to e\nu) = 0.1094 \pm 0.0045$. The full Run I results from CDF will be available shortly.

The DØ collaboration has recently completed a measurement of the ratio R. This study has almost 4 times the data sample (60k W's, 5k Z's), and expanded acceptance region and updated and detailed theoretical modeling. They measure $\mathrm{Br}(W \to e\nu) = 0.1066 \pm 0.0015 \pm 0.0021 \pm 0.0016$ (Δ = Measured - SM = -0.0018 ± 0.0030). Assuming that the width due to the electron is that expected from the SM (i.e, $\Gamma(W \to e\nu) = \Gamma(W \to e\nu)_{\mathrm{SM}}$) they extract $\Gamma(W) = 2.130 \pm 0.030 \pm 0.041 \pm 0.031$ GeV (Δ = Measured - SM = 0.036 ± 0.060 GeV). The results are compared with world measurements in Figure 11

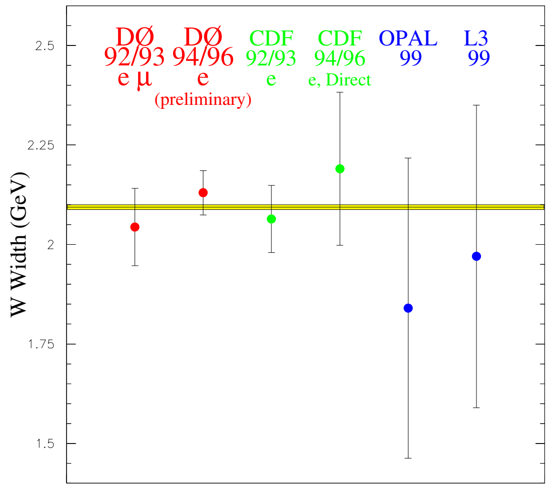

Figure 11: World measurements of the W width.

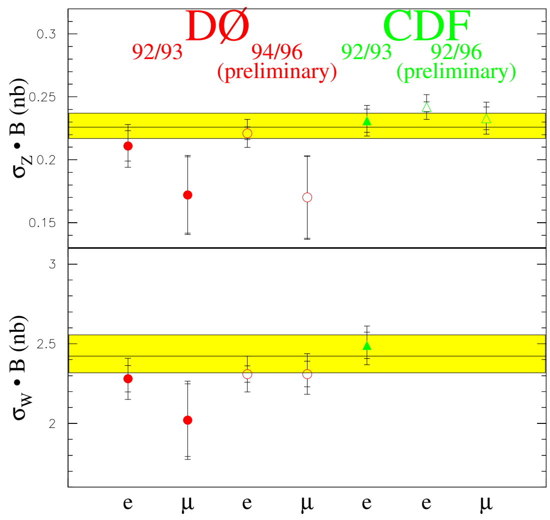

Figure 12: World measurements of the W and Z cross section at $\sqrt{s} = 1.8$ TeV.

3.3 Cross Section Results

There is a new DØ Result of the W and Z cross sections [13]. This new measurement is the world's most precise as it contains a high statistics sample as well as a new 5% measurement of the luminosity. Using the same samples as used to measure the ratio R they find $\sigma \cdot Br(Z^0 \rightarrow ee) = 221 \pm 3(stat) \pm \ 4(syst) \ \pm 10(lum)$ pb and $\sigma \cdot Br(W \rightarrow e\nu) = 2310 \pm 10(stat) \pm 50(syst) \pm 100(lum)$ pb. This new result is compared to other measurements in Figure 12.

In addition to the cross section measurement at $\sqrt{s} = 1.8\ TeV$, DØ has used a short run with $\sqrt{s} = 630$ GeV to make a second measurement of the W cross section. This measurement yields $\sigma(W \rightarrow e\nu)_{630\ \mathrm{GeV}} = 658 \pm 67$ pb which compares well with the other measurements from UA1 and UA2. See Figure 13. Putting these results together gives a measurement as a function of $\sqrt{s}$ as shown in Figure 14.

3.4 Measurement of the W Mass

A measurement of the W Mass is one of the most important tests of the Standard Model. This has been a premier measurement from the Tevatron for many years, and has recently been rivaled by LEP. It will continue to be a trademark of Run II physics. Again, leptonic

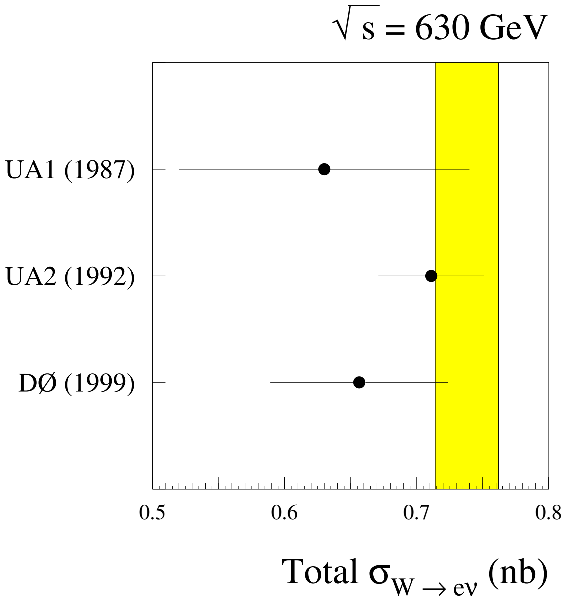

Figure 13: Measurements of the W cross section at $\sqrt{s} = 630$ GeV

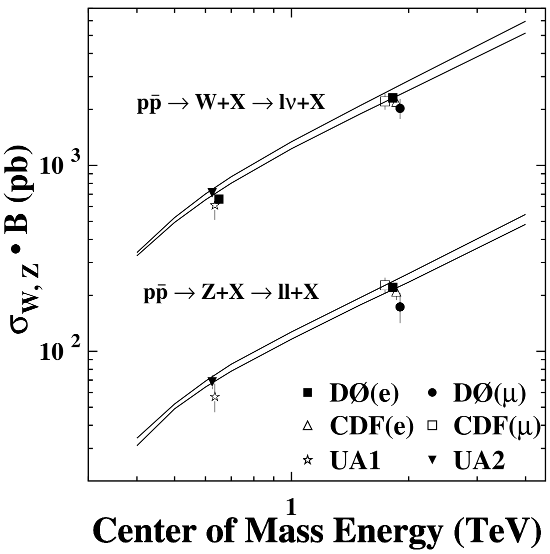

Figure 14: The $\sigma \cdot Br(W \to e\nu)$ and $\sigma \cdot Br(Z^0 \to e^+e^-)$ as a function of $\sqrt{s}$.

decays of the W are used and the mass is extracted from a measurement of the transverse mass lineshape. Both CDF and DØ have released recent measurements of the W mass; CDF in both the electron and muon channels (see Figures 15 and 16), and DØ in the central electron and forward electron channels.

Combining the individual measurements from CDF ($M_W = 80.43 \pm 0.08$ GeV) and DØ ($M_W = 80.47 \pm 0.09$ GeV) yields a Tevatron average of $M_W = 80.45 \pm 0.05$ GeV. Combining with the LEP average of 80.35 ± 0.06 GeV gives a world average of 80.39 ± 0.04 GeV. These results are summarized in Figure 17. These results are combined with the Tevatron measurement of the top quark mass in Figure 18. While these results are beginning to shed some real restrictions on the mass of the Higgs boson if the Standard Model is indeed correct, Run II should play a major role in this arena.

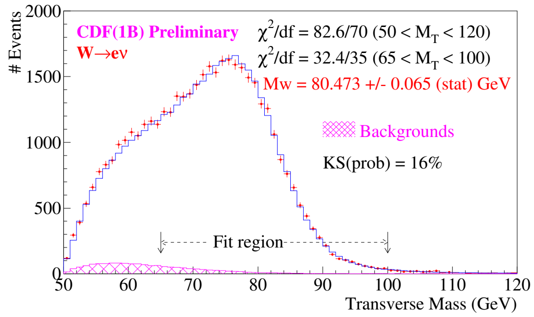

Figure 15: CDF measurement of the W transverse mass lineshape for use in the W mass measurement. This is the electron plot

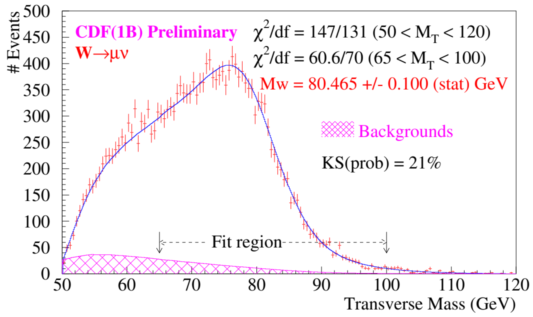

Figure 16: CDF measurement of the W transverse mass lineshape for use in the W mass measurement. This is the muon plot

4 The Future

The Tevatron continues to produce new physics results with the Run I data. With Run II is just around the corner we could very soon have a new set of hints to follow. There are major upgrades to the Tevatron: the center of mass energy will go from 1.8 TeV to 2.0 TeV and we are expecting total data samples on the order of 2 fb^{-1} which is a factor of 20 more data than we currently have. In addition both detectors are undergoing major upgrades. These include new central tracking chambers, silicon vertex detectors, improved muon coverage, faster readout electronics, high rate trigger and data acquisition systems. All of these should improve the acceptance for heavy objects (W, Z, top, Higgs, SUSY etc.) as well as improve the efficiency for b-tagging and τ identification.

It should be an exciting time for both measurements and searches. We expect to have measurements of the W mass to $\Delta M_W \approx 40$ MeV per experiment, $\Delta M_{top} \approx 3$ GeV per experiment, and have increased sensitivity to Higgs, SUSY, Technicolor or any other surprises which may come about.

5 Acknowledgments

The author would like to thank Gervasio Gomez, Sarah Eno, Dan Karmgard, Bill Ashmanskas, Darien Wood, and Mark Lancaster for their technical expertise and for providing

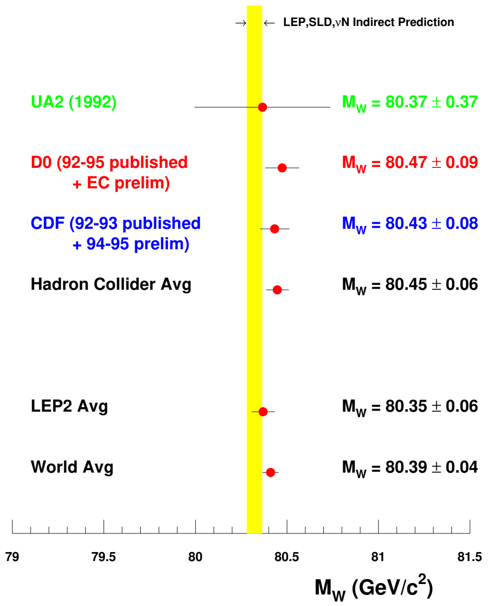

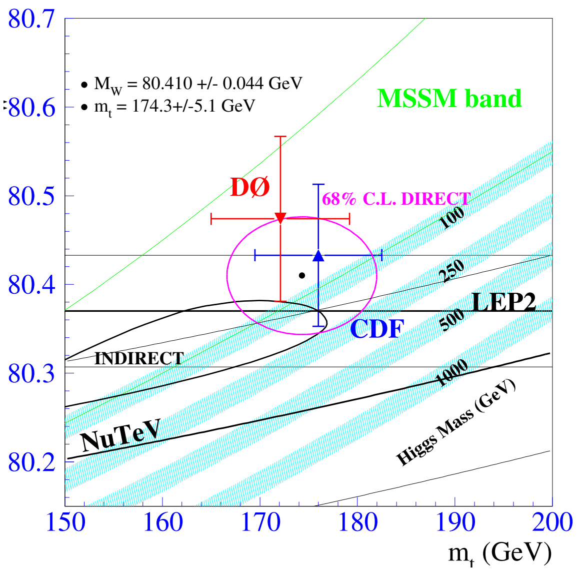

Figure 17: Values of the measured mass of the W boson at the Tevatron and LEP colliders.

Figure 18: The mass of the W boson as a function of the top quark mass. The circle represents the best estimate of the W mass as measured by the Tevatron and LEP. The top quark mass measurement is from the Tevatron alone.

many of the plots for this talk. The author would also like to thank Mike Gold for graciously agreeing to give this talk in addition to his own at the conference.

References

[1] J. C. Pati and A. Salam, *Phys. Rev.* D **10**, 275 (1994); E. Eichten *et al.*, *Phys. Rev.* D **34**, 1547 (1986); W. Buchmüller and D. Wyler, *Phys. Lett.* B **177**, 377 (1986) E. Eichten *et al.*, *Phys. Rev. Lett.* **50**, 811 (1983); H. Georgi and S. Glashow, *Phys. Rev. Lett.* **32**, 438 (1974).

[2] See, e.g., M. Leurer, *Phys. Rev.* D **49**, 333 (1994).

[3] M. Krämer *et al.*, *Phys. Rev. Lett.* **341**, 1997 (.)

[4] F. Abe, *et al.*, (CDF), Nucl. Instrum. Meth. **271A**.

[5] CDF Collaboration, F. Abe *et al.*, *Phys. Rev. Lett.* **81**, 4806 (1998).

[6] DØ Collaboration, S. Abachi, *et al.*, (DØ), Nucl. Instrum. Meth. **338A,** 185 (1994) and references therein.

[7] DØ Collaboration, B. Abbott *et al.*, Submitted to PRL, hep-ex/9904023.

[8] DØ Collaboration, P. C. Bhat, in *Proceedings of the 10th Topical Workshop on Proton-Antiproton Collider Physics,* edited by R. Raja and J. Yoh, p308 (AIP Press, 1995), and reference therein; JETNET v3.0 was used.

[9] B. Abbott *et al.*, to be submitted to PRL. For more details see D. Karmgard, Ph.D. Dissertation, The Florida State University, 1999.

[10] DØ Collaboration, B. Abbott *et al.*, *Phys. Rev. Lett.* **81**, 38 (1998)

[11] J. Blümlein, E. Boos, and A. Kryukov *Z. Phys.* C **76**, 137 (1997).

[12] CDF Collaboration, F. Abe *et al.*, *Phys. Rev.* D **52**, 2624 (1995).

[13] DØ Collaboration, B. Abbott *et al.*, to be submitted to Phys. Rev. D.